Weather and Climate Extremes 18 (2017) 44–54

Contents lists available at ScienceDirect

Weather and Climate Extremes

journal homepage: www.elsevier.com/locate/wace

Extreme value analysis of air pollution data and their comparison between two large urban regions of South America

Leila Droprinchinski Martins [a,f,*], Caroline Fernanda Hei Wikuats [a], Mauricio Nonato Capucim [a], Daniela S. de Almeida [a], Silvano Cesar da Costa [b], Taciana Albuquerque [c], Vanessa Silveira Barreto Carvalho [d], Edmilson Dias de Freitas [e], Maria de Fátima Andrade [e], Jorge Alberto Martins [a,f]

[a] Federal University of Technology, Paraná, Av. Dos Pioneiros, 3131, Londrina, 86047-125, Brazil
[b] State University of Londrina, Rodovia Celso Garcia, 86051-990, Londrina, Brazil
[c] Federal University of Minas Gerais, Department of Sanitary and Environmental Engineering, School of Engineering, Belo Horizonte, Brazil
[d] Federal University of Itajubá, Av. B.P.S, 1303, 37500903, Itajubá, Brazil
[e] Department of Atmospheric Sciences, University of São Paulo, Rua do Matão 1226, Cidade Universitária, 05508-090, São Paulo, Brazil
[f] Visiting Researcher at Lund University, Lund, Sweden

ARTICLE INFO

Keywords:
Air pollutants
Extreme events
Megacities
Ozone
Particulate matter

ABSTRACT

Sixteen years of hourly atmospheric pollutant data (1996–2011) in the Metropolitan Area of São Paulo (MASP), and seven years (2005–2011) of data measured in the Metropolitan Area of Rio de Janeiro (MARJ), were analyzed in order to study the extreme pollution events and their return period. In addition, the objective was to compare the air quality between the two largest Brazilian urban areas and provide information for decision makers, government agencies and civil society. Generalized Extreme Value (GEV) and Generalized Pareto Distribution (GPD) were applied to investigate the behavior of pollutants in these two regions. Although GEV and GPD are different approaches, they presented similar results. The probability of higher concentrations for CO, NO, NO_2, PM_{10} and $PM_{2.5}$ was more frequent during the winter, and O_3 episodes occur most frequently during summer in the MASP. On the other hand, there is no seasonally defined behavior in MARJ for pollutants, with O_3 presenting the shortest return period for high concentrations. In general, Ibirapuera and Campos Elísios stations present the highest probabilities of extreme events with high concentrations in MASP and MARJ, respectively. When the regions are compared, MASP presented higher probabilities of extreme events for all analyzed pollutants, except for NO; while O_3 and $PM_{2.5}$ are those with most frequent probabilities of presenting extreme episodes, in comparison other pollutants.

1. Introduction

Nowadays, over 50% of the world's population live in urban areas, and for Brazil, this population represents approximately 87%. (UN, 2014). Actually, high air pollutant's concentrations may be observed in a variety of places around the world as a result of substantial changes in land use as a consequence of urbanization, industrialization, extraction of natural resources, etc., and also due to energy demands. Therefore, Megacities pose a great concern, since they concentrate large populations and the air pollutants affect the health of those humans.

Atmospheric Particulate Matter (PM) and ozone (O_3) are the air pollutants that have received the most attention, since they cause several harmful effects on human health (WHO, 2013; Martins et al., 2009; Loomis et al., 2013; Xing et al., 2016), even when below air quality guidelines (WHO, 2013), and thus influencing the Earth's climate (Ravishankara, 2005; IPCC, 2014; Magrin et al., 2014). Nevertheless, the preparation and implementation of public policies is a challenge, mainly because urban areas are very different in terms of economy, social, cultural, and meteorological conditions within their respective regions.

The two largest urban areas in Brazil are the metropolitan areas of São Paulo and Rio de Janeiro and, according to the Study of Characterization and Trends of Urban Network in Brazil, these metropolises are inserted

* Corresponding author. Federal University of Technology – Paraná, Av. Dos Pioneiros, 3131, 86036-370, Londrina, Brazil.
E-mail address: leilamartins@utfpr.edu.br (L.D. Martins).

https://doi.org/10.1016/j.wace.2017.10.004
Received 19 May 2017; Received in revised form 14 September 2017; Accepted 31 October 2017
Available online 10 November 2017

whitin the global economy, presenting air quality issues http://www.observatoriodasmetropoles.ufrj.br/relat0082009.pdf (Paulino et al., 2010; Andrade et al., 2012, 2015; Mateus et al., 2013; Martins et al., 2015; Dominutti et al., 2016; Pereira et al., 2017). Recent studies have addressed the evolution of the pollutant concentrations and pointed to scientific gaps concerning air quality and emission sources in both the Metropolitan Area of São Paulo (MASP) (Kumar et al., 2016; Andrade et al., 2017) and also the Metropolitan Area of Rio de Janeiro (MARJ) (Gioda et al., 2016). However, a comparison between these two large Brazilian megacities, as well as the extreme value analysis, has never been made. MASP is the most important economic region in South America, with approximately 21 million people live; being the fifth most populous urban region in the world and the first in Latin America (UN, 2016). The region's urban area is located 700–900 m above sea level with ridges towering up to 1200 m. Its general topography is rather complex and the airflow is strongly influenced by local thermal circulations. The climate can be characterized by two predominant seasons: a wet one, which normally comprises the period from October to April, and a dry one, from May to September. The main source of pollutants in MASP is vehicular activity, since it has approximately 7 million vehicles burning gasohol (a mixture of 25–27% anhydrous ethanol and 75-73% gasoline), hydrated ethanol and diesel. The vehicle fleet is responsible for approximately 97% CO, 76% HC, 68% NO_X, 17% SOx, and 40% PM_{10} emissions (CETESB, 2017). Nowadays, more than 80% of the cars produced in Brazil are flex fuel (burning both ethanol and gasohol), which makes MASP atmosphere unique in terms of primary pollutants emissions (Carvalho et al., 2015). Industrial processes, according to the official inventory, are responsible for 3% CO, 24.2% HC (with 9.6% from liquid fuel evaporation), 32.4% NOx, 83% SOx and 10% PM_{10} emissions. The resuspension and secondary formation are equally responsible for the remaining 50% of PM_{10} emissions (CETESB, 2017).

MARJ is the second largest urban area in Brazil, covering 5327 square kilometers, and houses approximately 13 million people. It is also the twentieth most populous urban area in the world (United Nations, 2014). The region is composed of compact groups of mountains, deep valleys and lines of hills that divide wider or narrower plains (http://portalgeo.rio.rj.gov.br/bairroscariocas/texto_cidade.htm). It is located on the Brazilian east coast, presenting disorderly occupation and large bodies of water. The climate is characterized by a well-defined dry season, which occurs during the winter months, and a rainy season in the summer. MARJ has the second largest concentration of people, industries, vehicles and pollutant emission sources in Brazil. These factors tend to create local air pollution problems since the massifs of Tijuca and Pedra Branca, which are parallel to the coastline, act as physical barriers for the predominant sea winds, a condition that may influence the dispersion of pollutants (INEA, 2011). According to an inventory published by the *Fundação Estadual de Engenharia do Meio Ambiente* (FEEMA) in 2014, approximately 77% of atmospheric emissions in the region originate from vehicular sources (light and heavy-duty vehicles). The remaining 23% are from stationary sources, such as petrochemical, chemical, food, shipbuilding and energy transformation industries. Air pollution in urban areas may be addressed by a variety of statistical models, including Extreme Value Analysis (EVA). Such as many other phenomena covered by EVA, air pollutants are susceptible to events with unusually high concentrations in urban areas. The distribution of extreme values can usually be classified in one of three types: Gumbel, Fréchet and Weibull, which are referred to as Type I, Type II, and Type III, respectively, within the Generalized Extreme Value (GEV) distributions (Fisher and Tippett, 1928; Weibull, 1951; Jenkinson, 1955). GEV distributions use shape (ξ), location (μ) and scale (σ) parameters to fit the tails of a distribution. This modeling approach is used in environmental variables studies, such as rainfall and temperature data (Sangisolo, 2008; Panagoulia et al., 2014) and air pollutants concentrations (Smith, 1989; Küchenhoff and Thamerus, 1996; Lu, 2004; Ercelebi and Toros, 2009; Quintela-Del-Río and Francisco-Fernández, 2011; Su et al., 2012). The extensive use of the extreme value theory allows the prediction of the likelihood of the data studied within a given period, i.e., it assists in deciding if an extreme event is likely to occur. Another approach used in the study of the behavior of extreme values is the application of the Generalized Pareto Distribution (GPD) introduced by Pickands (1975), which is widely applied. This methodology involves the use of data that exceeds a certain threshold value, which is advantageous since it allows the analysis of all available data exceeding the threshold, without having to choose a group of maximum or minimum values, such as in the GEV theory.

In this work, EVA was applied to sixteen years (1996 to 2011) of hourly pollutant data measured in the MASP, and to seven years (2005 to 2011) of data measured in the MARJ. The probabilities of exceedance and the return period of high concentration of pollutant were calculated for carbon monoxide (CO), nitrogen oxides (NO and NO_2), O_3 and PM for both regions. In addition, a comparison in terms of pollutant concentrations between the two regions was performed.

2. Methodology

2.1. Description of the studied areas and their datasets

Sixteen years (1996 to 2011) of hourly O_3, NO, NO_2, CO and PM_{10} concentrations from eighteen stations located in MASP were analyzed to study the occurrence of O_3 and PM_{10} extreme values. In order to analyze $PM_{2.5}$, in the dataset available on MASP from 2011 (when automatic monitoring started) to 2014, two stations (Congonhas and IPEN-USP) were used. Pollutant hourly concentration data were compiled from the São Paulo State Environmental Agency (CETESB). In MARJ, there are several measuring stations, but only a few complete series are available. Therefore, seven years (2005 to 2011) of hourly data from the State Environmental Institute (INEA) measured at four stations were used in order to study O_3 and PM_{10} extreme values.

Fig. 1 shows the location of the stations in both MASP and MARJ. Tables 1 and 2 identify the stations and the studied pollutants in each mega-city, as well as provide a summary of basic statistics from the pollutant concentrations measured in each station. Among the stations analyzed in MASP, the highest average concentrations for PM_{10} and O_3 were found in stations 17 and 14, respectively. Congonhas station (2) presented the highest averages for NO, NO_2 and CO, due to the station's proximity to mobile sources. In MARJ, Campos Elísios (2) presented the highest average concentrations for PM_{10} and O_3.

Most stations in MASP (1–4; 8–9; 11–13 and 18) are highly impacted by vehicular emissions, while other stations (6–7; 10; 14–17) are influenced by both vehicular and industrial activities (CETESB, 2017). These different characteristics implicated in the concentrations of pollutants observed in each station. In MARJ, the Adalgisa Nery, Campos Elísios, Itaguaí and Jardim Primavera stations are located in areas characterized by urban and industrial expansion, and impacted by both vehicular and industrial emissions. Campos Elísios and Jardim Primavera are located in Duque de Caxias, a region that stands out due to its industrial production and petrochemical pole (INEA, 2011).

In order to perform the climatological characterization of MASP and MARJ, two stations from the National Institute of Meteorology were considered: São Paulo (23.30° S; 46.37° W) and Rio de Janeiro (22.53° S; 43.11° W). The annual cycle of mean monthly rainfall, relative humidity, air temperature, wind speed, nebulosity and sunshine duration for both stations are presented in Fig. 2 from 1961 to 1990.

It can be observed that both regions have rainy summers (Dec. to Mar.) and dry winters (Jun. to Sep.), with the highest precipitation values being recorded in São Paulo during the spring and summer (Fig. 2. B). The average annual precipitation of 1441 mm and 1070 mm were registered for São Paulo and Rio de Janeiro, respectively. In addition, relative humidity presented lower values during the winter months due to less precipitation in that period in both regions (Fig. 2 A). The monthly variability is not significant in other months in both regions, due to the proximity to the ocean; and even in the MASP, located approximately 70 km from the coastline, moisture transportation from the ocean is quite

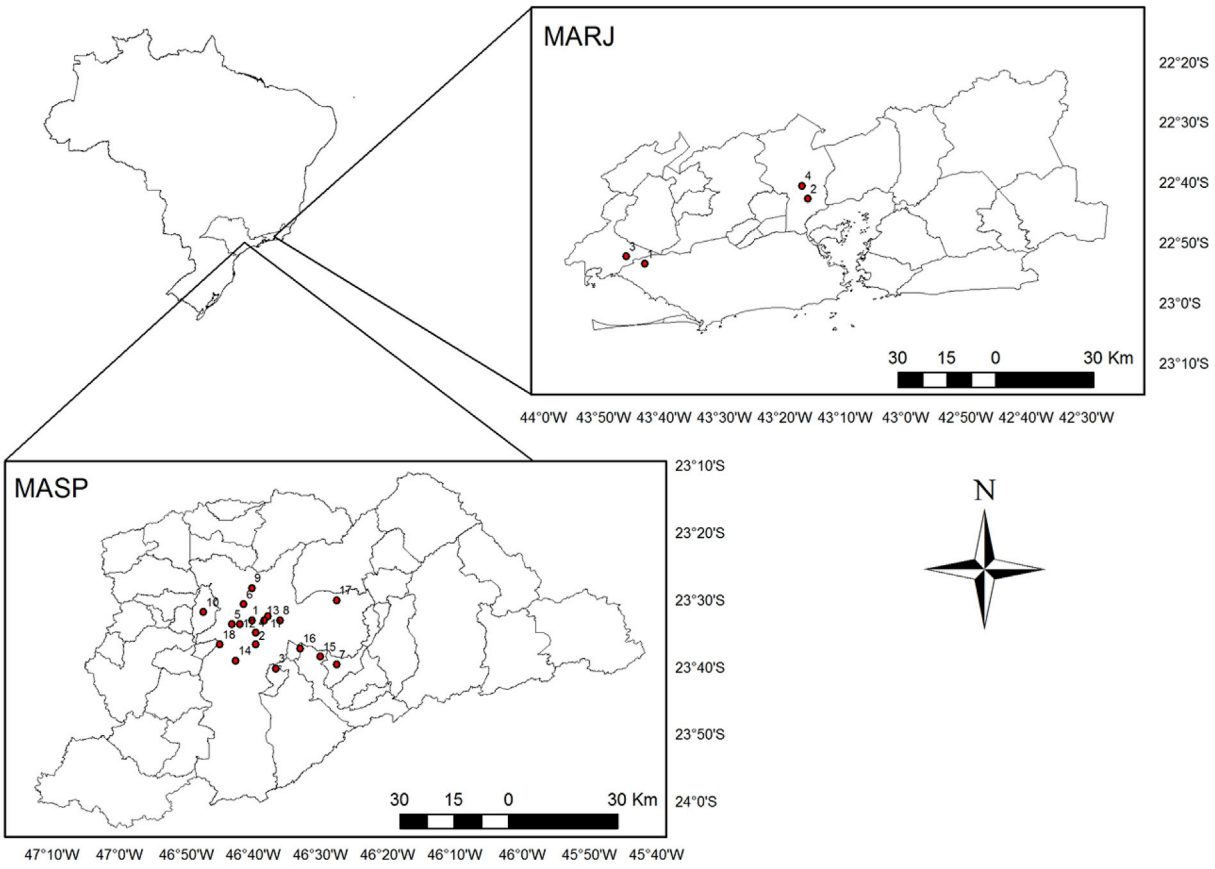

Fig. 1. Localization of air quality stations in the MASP and in the MARJ regions. Tables 1 and 2 show the names of stations and basic statistics parameters for the pollutants available for each station identified by number.

significant (Freitas et al., 2007).

Both regions present very similar air temperature patterns, with higher temperatures occurring from October/November to March (Fig. 2 C). Higher mean air temperature values are observed throughout the year in Rio de Janeiro. The months of May, June and July were the ones presenting the greatest differences in air temperature between the two studied regions. On average, the differences were around 4.5 °C. Therefore, the regions have different climate as observed in Fig. 2. São Paulo's subtropical climate is characterized by dry winters, and warm humid summers. Rio Janeiro's tropical climate has its winter drier than its summer, but with lower seasonal temperature variability than São Paulo (Alvares et al., 2014).

The Southeast of Brazil, where MASP and MARJ are located, is affected by different weather systems (South Atlantic Convergence Zone - SACZ, prefrontal instability lines, cold and warm fronts, high pressure system and sea breeze), with the SACZ being the most important system during the summer. In the winter, MASP is more greatly affected by cold fronts than MARJ. However, the presence of high-pressure systems in MASP may inhibit the entrance of cold fronts during winter, which in association with air mass subsidence, inhibits cloud formation (Freitas et al., 2007; Lima et al., 2010; Silva Dias et al., 2013).

2.2. Applied statistical analyses

This work used EVA as statistical treatment. EVA was used to estimate the probability of unusual pollution peaks. Even short-term exposure to air pollutant peaks can cause serious health diseases to the population. Therefore, EVA can be seen as an important tool in order to assess the incidence of pollution peaks to which a given population is exposed. Two approaches were used: the first one is the Generalized Extreme Value distribution (GEV), which was applied to the monthly maximum hourly concentration measures (Fisher and Tippett, 1928; Weibull, 1951; Jenkinson, 1955; Ercelebi and Toros, 2009); the second approach used herein is the Generalized Pareto Distribution (GPD), often used to model the tails of another distribution, composed of values above a threshold (Pickands, 1975).

GEV is defined by three parameters related to the behavior of a distribution tail: shape (ξ), location (μ) and scale (σ). The value of the shape (ξ) parameter defines three specific types of distribution: Gumbel ($\xi \to 0$), Fréchet ($\xi > 0$) or Weibull ($\xi < 0$) (Jenkinson, 1955). GPD uses the shape (ε) and scale (σ) parameters to define the distribution, and the shape parameter has an important impact on the character of the distribution. It can be classified as Pareto type II distribution if $\varepsilon < 0$; usual Pareto distribution if $\varepsilon > 0$; and Exponential if $\varepsilon \to 0$ (McNeil and Saladin, 1997; Dominutti et al., 2016). The Pareto distribution can be used to model several phenomena, such as size of cities, the highest one-day rainfall in one year, number of hectares of forest affected by a fire, etc.

Many of the factors that influence atmospheric pollutant concentrations are related to weather conditions, whose variations cannot be captured by studying only the maxima over extensive periods (Piegorsch et al., 1998). Therefore, the theory is applied to the daily maxima over a threshold by using GPD, and monthly maxima data by using GEV. In addition, one of the conditions for obtaining satisfactory statistical conclusions in the application of the extreme value theory is that the sample data must be independent and identically distributed (i.i.d) (Roberts, 1979; Georgopoulos and Seinfeld, 1982). In the first case, the time series is not stationary and has no autocorrelation, and the second case is related to the probability density function that is constant in time (Sharma et al., 1999).

The monthly maxima values were gathered in to two clusters for the entire MASP data period, which presented a well-defined seasonal behavior for all pollutant concentrations in the 18 analyzed stations.

Table 1
Air quality stations in MASP, measured pollutants concentrations and basic statistic parameters from the 1996 to 2011 dataset.

ID	Station	Pollutants[a]	Average	S. D.	Max.	Min.
1	Cerqueira César	NO	72.43	85.54	1028.44	0.02
		NO_2	63.36	34.16	492.24	0
		CO	1.48	1.18	15.16	0.01
2	Congonhas	NO	157.86	145.41	1807.73	0.07
		NO_2	74.40	40.60	499.75	0.13
		CO	2.27	1.65	24.3	0.01
		$PM_{2.5}$	21.49	14.31	160.42	0.05
3	Diadema	O_3	34.04	31.03	314.26	0.18
		PM_{10}	44.67	34.49	1084.98	0.02
4	Ibirapuera	NO	21.20	56.24	1107.03	0
		NO_2	42.81	27.78	486.98	0
		CO	0.91	0.86	18.51	0
		O_3	36.87	37.56	402.84	0.03
		PM_{10}	40.95	34.73	961.40	0.07
5	IPEN-USP	$PM_{2.5}$	16.62	15.33	152	0.15
6	Lapa	NO	162.11	188.92	1332.78	0
		NO_2	53.11	37.01	334.97	0.02
		CO	1.87	1.50	12.1	0.02
7	Mauá	NO	10.06	25.07	578.10	0
		NO_2	30.37	21.07	327.12	0.74
		O_3	38.53	34.17	380.57	0.05
		PM_{10}	38.19	31.58	769.94	0.01
8	Mooca	O_3	30.12	32.15	342.33	0.01
		PM_{10}	39.34	32.99	831.50	0.01
9	Nossa Senhora do Ó	O_3	28.62	32.93	279.37	0
		PM_{10}	40.82	31.81	478.71	0.06
10	Osasco	NO	105.83	89.79	895.50	0
		NO_2	62.45	30.19	461.23	0.01
		CO	2.06	1.26	16.91	0.01
11	Parque D. Pedro II	NO	54.30	80.33	1129.06	0.02
		NO_2	55.33	31.65	390.78	0
		CO	1.27	1.10	18.46	0
		O_3	25.29	28.23	290.77	0.01
		PM_{10}	43.74	37.43	632.47	0.01
12	Pinheiros	NO	57.25	111.94	1268.96	0.06
		NO_2	42.72	29.61	464.37	0.01
		CO	1.09	1.04	14.38	0.0
		O_3	24.73	27.05	383.89	0.01
		PM_{10}	46.83	36.62	469.62	0.05
13	Santana	O_3	36.93	35.08	412.28	0.09
		PM_{10}	47.44	34.73	377.04	0.01
14	Santo Amaro	CO	0.92	0.84	13.11	0.04
		O_3	40.05	34.60	390.04	0.01
		PM_{10}	46.71	38.40	472.77	0.02
15	Santo André - Capuava	O_3	35.00	30.99	311.58	0.01
		PM_{10}	38.06	28.66	443.28	0.01
16	São Caetano do Sul	NO	43.05	70.09	1167.80	0
		NO_2	50.50	29.35	437.24	0.14
		CO	1.24	1.25	26.34	0.01
		O_3	37.88	32.95	381.24	0.02
		PM_{10}	41.40	32.60	557.32	0.01
17	São Miguel Paulista	O_3	36.22	30.37	279.00	0.02
		PM_{10}	51.60	41.16	589.74	0.01
18	Taboão da Serra	NO	62.15	98.84	953.16	0.01
		NO_2	45.14	23.46	287.79	0.01
		CO	1.39	1.25	13.84	0.05

[a] O_3, NO, NO_2, PM_{10} and $PM_{2.5}$ in μg m^{-3}; CO in ppm; $PM_{2.5}$ from 2011 to 2014.

Cluster 1 (C1) ranges from May to August (winter), while cluster 2 (C2) goes from September to April (summer). Therefore, the dataset was split in to two seasons and fit two different extreme values models to satisfy the i. i.d. condition. This approach was also performed, for instance, by Küchenhoff and Thamerus (1996). The data analyzed from MARJ did not show a very pronounced seasonal pattern for all pollutant concentrations as seen at MASP, and therefore they were not grouped. These different patterns between the regions are mainly due to the aforementioned climatic differences.

In order to perform an analysis using the GPD, an important practical issue is the selection of the threshold. In this case, a 95% quantile was used for choosing the threshold, which was obtained from the daily maxima. Since the two regions have different concentration values, the threshold value is different for each pollutant at each station.

Table 2
Air quality stations in MARJ, measured pollutants concentrations and basic statistic parameters from the 2005 to 2011 dataset.

ID	Station	Pollutants[a]	Average	S. D.	Max.	Min.
1	Adalgisa Nery	O_3	37.01	26.71	185.01	0.005
		PM_{10}	29.85	20.14	344.41	0.3
2	Campos Elísios	O_3	41.04	41.40	431.49	0.005
		PM_{10}	46.94	34.64	426.92	0.58
3	Itaguaí – Monte Serrat	O_3	34.91	24.18	178.91	0.005
		PM_{10}	31.71	21.43	304.63	0.63
4	Jardim Primavera	NO	39.45	43.30	613.66	0.58
		NO_2	35.31	24.22	313.84	0.92
		CO	0.60	0.30	12.11	0.05
		O_3	35.46	37.61	511.13	0.05
		PM_{10}	36.09	29.51	469.81	0.04

[a] O_3, NO, NO_2 and PM_{10} in μg m^{-3}, CO in ppm.

2.3. Probability and return period

The probability of concentrations occurring above thresholds and of presenting return period was calculated using the National Air Quality Standard as a reference, and the limits recommended by the World Health Organization (WHO). The return period is the estimated time of occurrence of peak levels above thresholds for O_3, PM_{10} and $PM_{2.5}$, which was calculated for all stations analyzed in MASP and MARJ in order to find the stations with the highest probability of extreme values. Although distribution shape parameter may help identify the places with greater chance of extreme concentrations, the probability is also influenced by other distribution parameters. In this work, the probability and return period were only calculated for the GEV approach, since it fitted two seasons in MASP. The following equation (1) was used (Bautista, 2002):

$$p = 1 - \exp\left\{ - \left[1 + \xi\left(\frac{x-\mu}{\sigma}\right)\right]^{-\frac{1}{\xi}}\right\} \quad (1)$$

where (x) is the threshold value when $\xi \neq 0$; (μ) and (σ) are the location and scale parameters; (p) is theprobability ($t = \frac{1}{p}$), and (t) is the return period.

3. Results and discussion

3.1. Extreme value analysis

Figs. 3 and 4 show examples of plots obtained from the application of the GEV approach for Ibirapuera (4) and Congonhas (2) stations, located in MASP, and Jardim Primavera (4) station located in MARJ. The plots are for PM_{10}, $PM_{2.5}$ and O_3 in both clusters C1 (winter) and C2 (summer) in the case of MASP. The discussion focus on PM_{10}, $PM_{2.5}$ and O_3, since they are the regular pollutants of the greatest concern in both regions (Martins et al., 2015; Kumar et al., 2016; Gioda et al., 2016; Andrade et al., 2017).

The probability plots show the empirical probabilities in the x axis, with the model probabilities observed in the y axis. A good model that fits the graphics should have a linear behavior as observed in Figs. 3 and 4. The empirical data presented good fitting for both approaches - GEV and GPD. The Figures also show the return periods (in years) for several concentrations. PM_{10} concentrations of 150–300 μg m^{-3} are frequent in C1, while in C2 the concentrations are in the range of 100–200 μg m^{-3}. $PM_{2.5}$ concentrations follow the same behavior as PM_{10} in relation to winter and summer. On the other hand, O_3 presented an opposite behavior, with O_3 concentrations in the range of 100–150 μg m^{-3} in C1, and 150–250 μg m^{-3} in C2. These behaviors are associated with the different meteorological conditions observed during summer and winter,

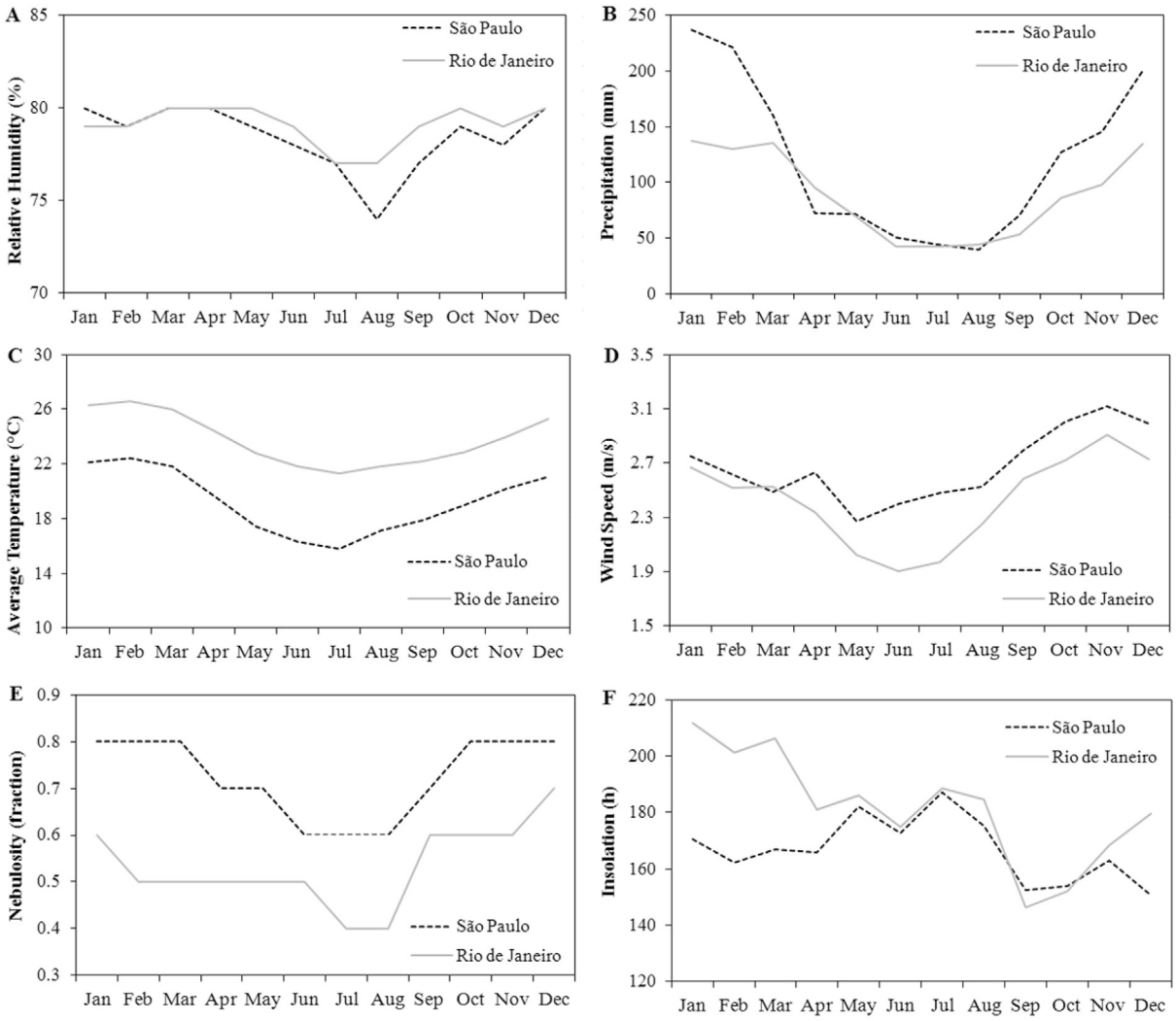

Fig. 2. Annual cycle of monthly mean precipitation (A), relative humidity (B), average temperature (C), wind speed (D), nebulosity (E) and insolation (F) for Rio de Janeiro and São Paulo.

as already mentioned. The probabilities and the return periods for these pollutants are discussed in a specific topic presented below.

Table 3 shows scale (σ), shape (ξ) and number (N) parameters exceeding the GPD distribution threshold (95% quantile) fitted for MASP stations for PM_{10}, $PM_{2.5}$, and O_3. The location, scale and shape parameters of the GEV distribution fitted for MASP in both groups (C1 and C2), and for MARJ for all pollutants analyzed are presented as supplementary material (Tables S1-S5). In the GPD approach, the shape (ε) parameter demonstrates the tail model of the curve where if $\varepsilon < 0$, the model can be considered as having a light (mild) tail; if $\varepsilon > 0$, the model is considered as having a heavy tail, which indicates greater likelihood of extreme values (Pickands, 1975).

In MASP, by analyzing the GPD results, it could be observed that, for PM_{10}, most of the stations showed a heavy tail model with $\varepsilon > 0$, with station 4 (Ibirapuera) presenting the highest number of exceedances (N) followed by station 11 (Parque Dom Pedro II). For O_3, half of the stations presented a light tail model and the other half presented heavy tails, with the highest number of exceedances to the threshold occurring in station 4. The results from GEV (please refer to the supplementary material) and GPD agree, indicating that station 4 presented the highest shape value for O_3, and therefore, it is the station that may present extreme concentrations for that pollutant. For PM_{10}, from GEV results, the higher shape parameter values were found in station 9 (Fréchet type, $\xi = 0.37$) in C1 and station 4 in C2 (Fréchet type, $\xi = 0.34$), which also agree with the GPD results. For $PM_{2.5}$, station 2 showed a light tail model, since the ε value is less than 0. Station 5 presented a heavy tail model, with $\varepsilon > 0$. However, station 2 presented the highest number of exceedances (N) to the threshold. In addition, based in GEV results (see Table S1), the location parameter (μ) is higher in station 2 ($\mu = 107.01$ in C1 and $\mu = 62.48$ in C2) when compared with station 5 ($\mu = 90.55$ in C1 and $\mu = 51.55$ in C2), as well as in relation to C1 (winter) and C2 (summer).

In MARJ, only four stations were analyzed due to the lack of available data, consideringthe criterion of 80% valid data. Table 4 shows the GPD parameters for MARJ stations. For PM_{10}, there are positive and negative values of ε for the same number of stations (2 stations) and therefore, there is no predominant distribution for this pollutant. However, for O_3, only station 4 presented a heavy tail model, indicating the highest number of exceedances (N) to the threshold in this station. For O_3, according to the results obtained from the GEV approach, both stations 4 and 2 presented similar distribution parameters, indicating that both may have high probabilities to extreme events.

3.2. Probability and return period

The probabilities of having concentrations above thresholds (in μg m^{-3}) and the return periods (in years) for the extreme values were calculated for O_3, PM_{10} and $PM_{2.5}$, and are shown in Tables 5 and 6, for MASP and MARJ, respectively. The highest probabilities for O_3, PM_{10} and $PM_{2.5}$ among stations are highlighted. As previously mentioned, O_3 and PM are the pollutants of main concern in urban areas, and therefore,

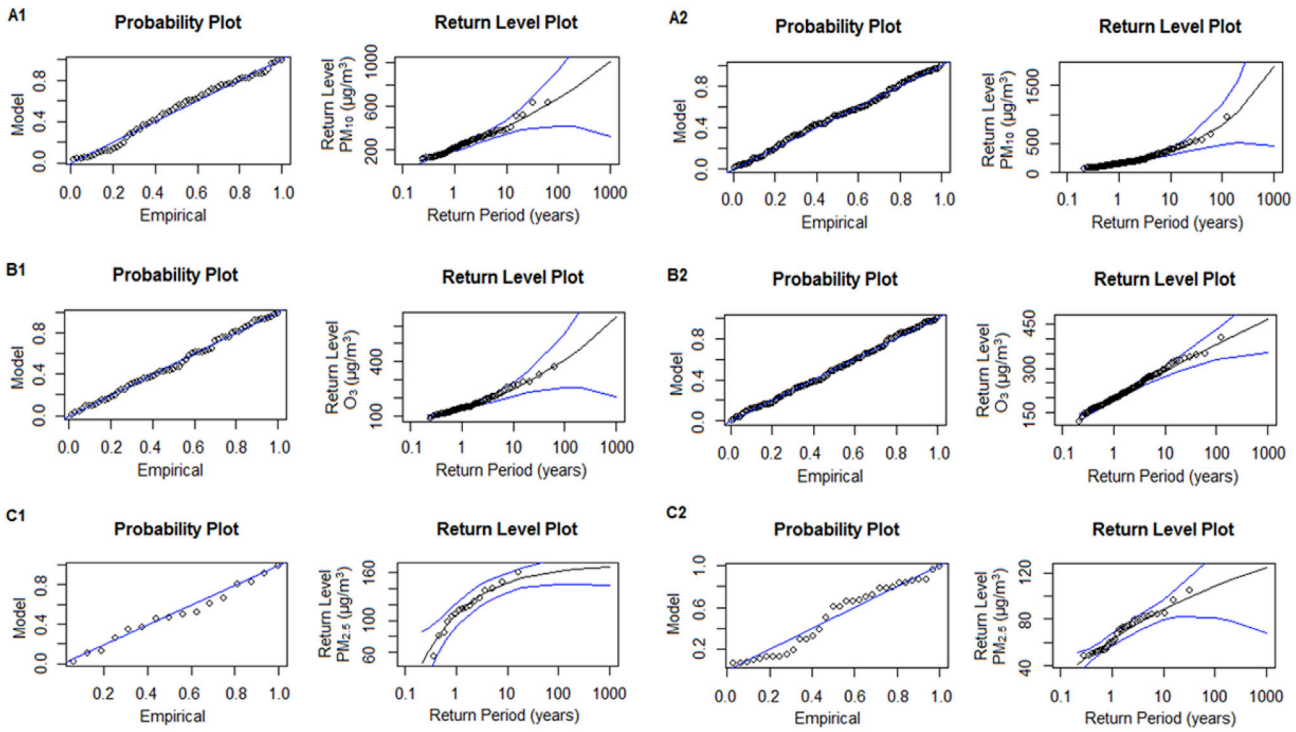

Fig. 3. Model adjustment and return periods graphics. Ibirapuera station for PM_{10} in cluster 1 (A1) and cluster 2 (A2); and for O_3 in cluster 1 (B1) and cluster 2 (B2). . Congonhas station for $PM_{2.5}$ in cluster 1 (C1) and cluster 2 (C2).

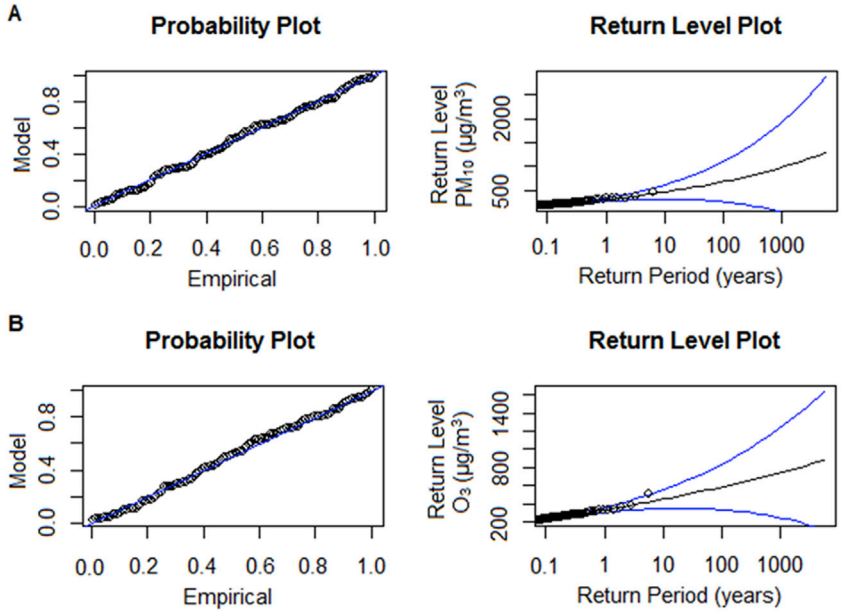

Fig. 4. Model adjustment and return periods graphics for Jardim Primavera station, in MARJ, for PM_{10} (A) and O_3 (B).

the analysis was focused on them.

The probability of the occurence of extreme concentrations significantly differs between winter and summer, as expected, in MASP. For PM_{10} and $PM_{2.5}$, the highest probabilities appear during winter (C1) for stations 17 (São Miguel Paulista) and 2 (Congonhas), respectively. The return periods of concentrations above 250 µg m^{-3} and 100 µg m^{-3} are of 1.2 and 1.4 years, for PM_{10} and $PM_{2.5}$, respectively. For example, in 2015, many days (24-h average) registered values above 50 µg m^{-3} for $PM_{2.5}$, which is twice the level recommended by WHO.

For ozone, differently from the particles, the highest probabilities occur during summer (C2) for stations 4 (Ibirapuera) and 14 (Santo Amaro) followed by station 7 (Mauá), in MASP. Additionally, hourly concentrations above 200 µg m^{-3} could occur, with a return period of 1.6 years at both stations 4 and 14. High concentrations were evidenced in 2015, such as 199 µg m^{-3} for 8 h average, and 268 µg m^{-3} for 1 h average at station 4.

Table 3
GPD parameters of scale (σ) and shape (ε) estimated for PM_{10}, O_3 and $PM_{2.5}$ concentrations at MASP stations.

ID	PM_{10}			O_3			$PM_{2.5}$		
	σ	ε	[a]N	σ	ε	N	σ	ε	N
1	–	–	–	–	–	–	–	–	–
2	–	–	–	–	–	–	27.72	−0.46	70
3	47.06	0.12	253	30.99	−0.02	224	–	–	–
4	64.03	0.13	273	35.70	0.03	277	–	–	–
5	–	–	–	–	–	–	12.50	0.05	51
6	–	–	–	–	–	–	–	–	–
7	73.22	0.14	203	33.57	−0.08	258	–	–	–
8	49.06	0.12	164	45.46	−0.13	259	–	–	–
9	51.48	−0.04	226	24.88	0.04	132	–	–	–
10	–	–	–	–	–	–	–	–	–
11	52.30	0.17	269	34.14	−0.10	240	–	–	–
12	35.41	0.11	165	22.98	0.22	204	–	–	–
13	32.64	0.09	203	33.90	0.04	217	–	–	–
14	44.49	0.02	234	35.52	−0.06	129	–	–	–
15	37.17	0.11	263	27.38	0.03	190	–	–	–
16	57.20	−0.02	251	27.43	0.06	255	–	–	–
17	75.05	−0.20	130	43.76	−0.24	146	–	–	–
18	–	–	–	–	–	–	–	–	–

[a] N = number of exceedances above threshold.

Table 4
GPD parameters of scale (σ) and shape (ε) estimated for PM_{10} and O_3 concentrations at MARJ stations.

ID	PM_{10}			O_3		
	σ	ε	[a]N	σ	ε	N
1	31.56	0.23	52	21.34	−0.10	52
2	53.50	−0.03	88	49.59	−0.08	85
3	58.56	−0.19	51	22.84	−0.26	53
4	37.84	0.16	113	38.64	0.08	103

[a] N = number of exceedances above threshold.

In MARJ, the highest probability of extreme values for O_3 is observed in stations 2 and 4, while for PM_{10}, it was only observed in station 2. These two stations are the ones presenting the lowest return period for the occurrence of extreme concentrations for O_3 and PM_{10}. For instance, the return period for an O_3 concentration episode above 200 μg m^{-3} is of 1.4 years at station 2. In addition, it is the pollutant with the highest frequency of extreme events among those analyzed in MARJ.

3.3. Comparison between the megacities

In order to evaluate the seasonal behavior of pollutants and compare the magnitude of concentrations between the two metropolitan areas, monthly average concentrations were calculated in two stations which had more than 80% of valid data through the 2005 to 2011 period. MASP presented the highest concentrations for CO and NO_2 in relation to MARJ. NO and PM_{10} (except for Jul. and Sep.) presented the highest concentrations in MARJ, probably due to stationary sources, such as petrochemicals, that are located close to that station. O_3 presented specific behavior, with higher concentrations from January to June in MARJ and from August to December in MASP. In addition, for O_3 the probabilities and return periods were similar for both São Paulo and Rio de Janeiro.

MASP presented a well-defined seasonal behavior, with higher

Table 5
Probability of concentrations occurring above thresholds and the return period (years) for extreme value for MASP.

Stations	O_3 (μg m^{-3})					PM_{10} (μg m^{-3})					$PM_{2.5}$ (μg m^{-3})				
	P[a] (100)		P (140)		t[b] (200)	P (50)		P (150)		t (250)	P (25)		P (60)		t (100)
	[c]C1	[d]C2	C1	C2	C2	C1	C2	C1	C2	C1	C1	C2	C1	C2	C1
1	–	–	–	–	–	–	–	–	–	–	-	-	-	-	-
2	–	–	–	–	–	–	–	–	–	–	**0.999**	**1**	**0.971**	**0.703**	**1.4**
3	0.871	0.998	0.518	0.923	2.3	1	0.999	0.808	0.561	4.3	–	–	–	–	–
4	**0.977**	**1**	**0.667**	**0.981**	**1.6**	1	1	0.885	0.594	2.2	–	–	–	–	–
5	–	–	–	–	–	–	–	–	–	–	1	1	0.961	0.434	2.1
6	–	–	–	–	–	–	–	–	–	–	–	–	–	–	–
7	0.964	1	0.680	0.971	1.9	1	1	0.934	0.644	2.5	–		–	–	–
8	0.863	0.990	0.477	0.878	2.2	0.998	1	0.826	0.536	2.9	–		–	–	–
9	0.824	0.988	0.263	0.807	4.0	1	1	0.731	0.471	6.3	–	–	–	–	–
10	–	–	–	–	–	–	–	–	–	–	–	–	–	–	–
11	0.781	0.934	0.428	0.734	3.7	0.999	0.998	0.891	0.627	2.0	–	–	–	–	–
12	0.720	0.972	0.291	0.729	3.9	1	0.995	0.944	0.639	2.7	–	–	–	–	–
13	0.936	0.998	0.571	0.929	2.0	1	1	0.834	0.458	6.8	–	–	–	–	–
14	0.876	**1**	0.538	**0.981**	**1.6**	1	0.994	0.956	0.722	2.4	–	–	–	–	–
15	0.876	0.980	0.491	0.824	3.0	1	1	0.818	0.569	5.9	–	–	–	–	–
16	0.874	0.999	0.574	0.936	2.2	1	1	0.913	0.477	2.9	–	–	–	–	–
17	0.930	0.968	0.548	0.841	2.5	**1**	**1**	**0.997**	**0.730**	**1.2**	–	–	–	–	–
18	–	–	–	–	–	-	-	-	-	-	–	–	–	–	–

[a] P = Probability of concentrations occurring above threshold value.
[b] t = return period in years for cluster with the highest probability of extreme values.
[c] C1 = winter.
[d] C2 = summer.

Table 6
Probability of concentrations occurring above thresholds and the return period (years) for extreme value for MARJ.

Stations	O_3 (μg m^{-3})			PM_{10} (μg m^{-3})		
	P[a] (100)	P (140)	t[b] (200)	P (50)	P (150)	t (250)
1	0.803	0.260	76.5	0.997	0.364	14.1
2	**0.991**	**0.941**	**1.4**	**1**	**0.694**	**5.9**
3	0.726	0.241	∞	0.978	0.321	14.6
4	0.983	0.910	1.6	0.951	0.511	7.5

[a] P = Probability of concentrations occurring above threshold value.
[b] t = return period in years for cluster with the highest probability of extreme values; (∞) high return period.

concentrations of CO, NO, NO_2 and PM_{10} during winter, and O_3 in spring and summer, as presented in Fig. 5. During the winter months (June, July and August), the entrance of cold fronts is inhibited and causes thermal inversion at low levels of the troposphere, generating a high concentration of pollutants in MASP. Thermal inversions occur near the surface with a higher frequency, and the pollutants stagnate close to the ground. All these features make pollution dispersion more difficult. This is different for O_3, with many studies reporting that high O_3 concentrations at the surface are related with high pressure systems (i.e. ASAS), clear sky conditions and high temperatures (Comrie and Yarnal, 1992; Jenkin et al., 2002; Cooper et al., 2015). Summer provides higher temperatures and higher incidence of solar radiation, but the presence of clouds can change the solar radiation flux, thus reducing the photochemical reactions responsible for the ozone formation in MASP (Sánchez-Ccoyllo et al., 2006; Martins and Andrade, 2008; Carvalho et al., 2015).

The pollutant concentrations do not reflect a well-defined seasonal pattern in MARJ as observed in MASP. For example, the monthly average CO concentrations in Jardim Primavera did not change significantly throughout the year, and O_3 presented its peak in February. It can be observed that the highest values of O_3 concentration occur in the spring months in MASP (from September to December) and in the summer months in MARJ (between January and March), as shown in Fig. 5. This is probably due to the decrease in the cloud cover in MARJ in the months of January and February, increasing the ozone formation; while in MASP the nebulosity increases in summer afternoons and is lower during spring months. These different patterns are consistent with the climatology of the regions.

In addition, frequency distribution charts for the hourly concentrations (2005 to 2011) were made for both regions, in order to compare the frequency distribution of concentration, which are shown in Fig. 6. The O_3 and NO_2 distribution profiles are very similar in both regions, with the highest frequency observed in the range of low concentrations in Jardim Primavera station (Fig. 6 B and D). That particular behavior can be

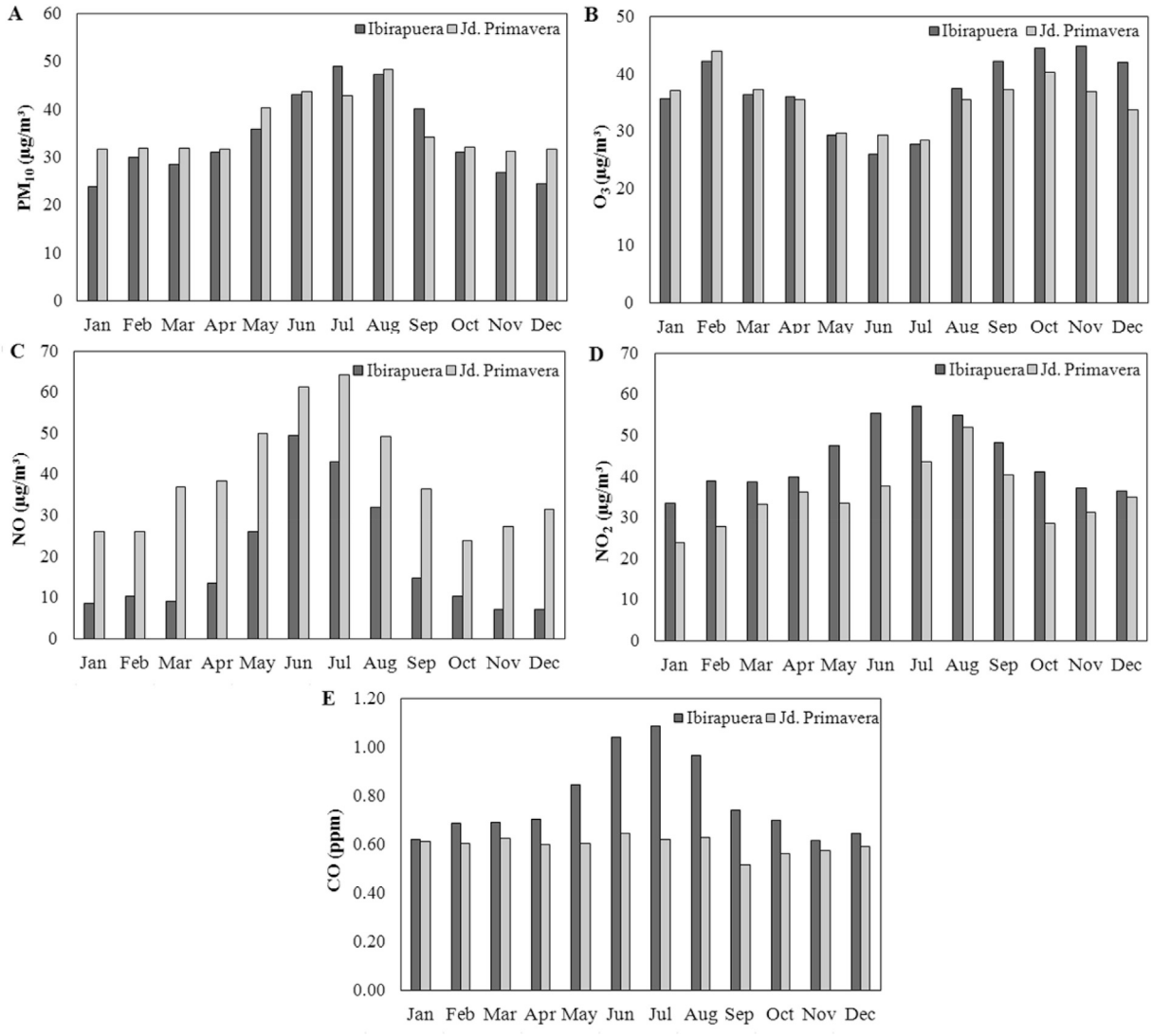

Fig. 5. Monthly mean concentrations of PM_{10} (A), O_3 (B), NO (C), NO_2 (D) and CO (E) in Ibirapuera and Jardim Primavera stations from 2005 to 2011.

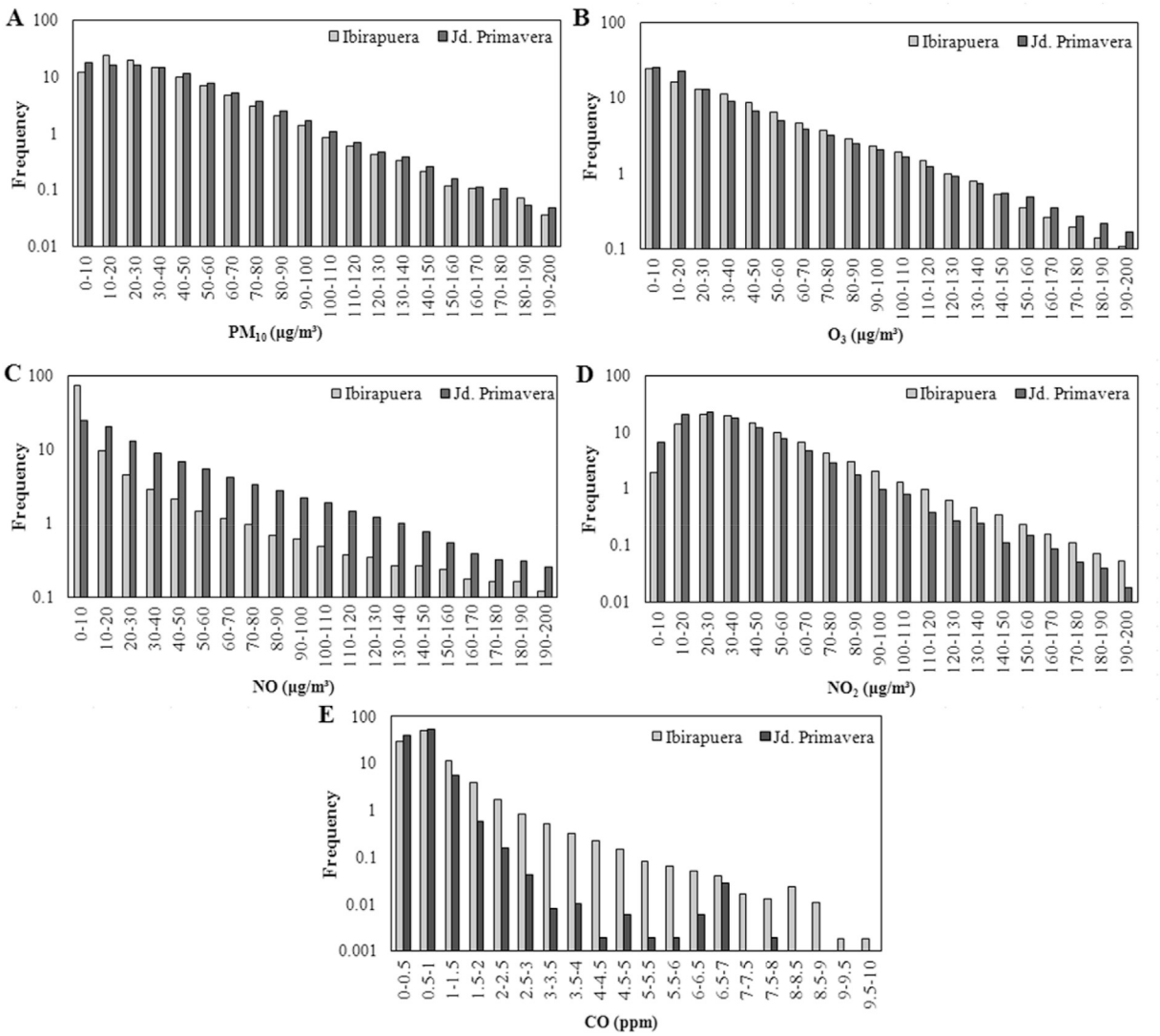

Fig. 6. Frequency distribution of PM_{10} (A), O_3 (B), NO (C), NO_2 (D) and CO (E) concentrations in Ibirapuera and Jardim Primavera stations from 2005 to 2011.

observed for O_3 in the range above the value of 140 µg m^{-3}, in which Jardim Primavera station still presented a high frequency of occurrences. For PM_{10} (Fig. 6 A), the frequency distribution profile is also similar, but with slightly higher frequency in the intermediate/high range concentration values of up to 180 µg m^{-3} in Jardim Primavera station.

The profile with the most difference were registered for the pollutants NO and CO (Fig. 6 C and E). For the first one, Ibirapuera is the station with the highest value in the low range of concentrations, while Jardim Primavera exceeds Ibirapuera in the concentration of 20 µg m^{-3} to become the station with the highest frequency of occurrence in other concentration ranges. For CO, Jardim Primavera station presented a different behavior with a significant drop followed by various highs and lows in the frequency of occurrence. However, Ibirapuera presented a profile that showed an increase and then a soft decrease in the frequency from the 1.5-ppm concentration, becoming the station with the highest values in the intermediate/high range of concentrations, thus indicating a great influence of vehicular emissions.

Fig. 7 shows the typical daily profile (Fig. 7A and B) and frequency for hourly $PM_{2.5}$ concentrations in two São Paulo stations from 2011 to 2014 (Fig. 7 C). The station profiles are different, but present higher concentrations in the evening and around midnight due to (a) higher humidity at that time, promoting the growth of particles; and (b) the lower height of the boundary layer. A preeminent peak is observed around 10:00–11:00 a.m. only at IPEN-USP station, which may be associated with the transport of particles emitted earlier mainly by heavy-duty vehicles burning diesel. There are important highways relatively close to that station, crossing MASP from West to East, with an intense flow of vehicles.

The frequency of $PM_{2.5}$ concentrations is higher for lower concentrations, but concentrations from 50 to 60 µg m^{-3} are very common in both stations, with almost half of the data in that range. The frequency of extreme concentrations is higher at the Congonhas station than at the IPEN-USP, with values of up to 130 µg m^{-3}.

4. Concluding remarks

The extreme value analysis allows modeling data through mathematical functions, and allows the use of these equations to estimate, even for short periods, the values that can be expected in the coming years. In this way, some converging results were found even from two different approaches in extreme values.

In MASP, the probabilities of occurring concentration above thresholds for CO, NO, NO_2, PM_{10} and $PM_{2.5}$ are more frequent during the winter (C1), while for O_3, these are more frequent in the summer (C2). Ibirapuera station in general presented the highest probabilities of extreme events in MASP. In MARJ, although only a few stations could be

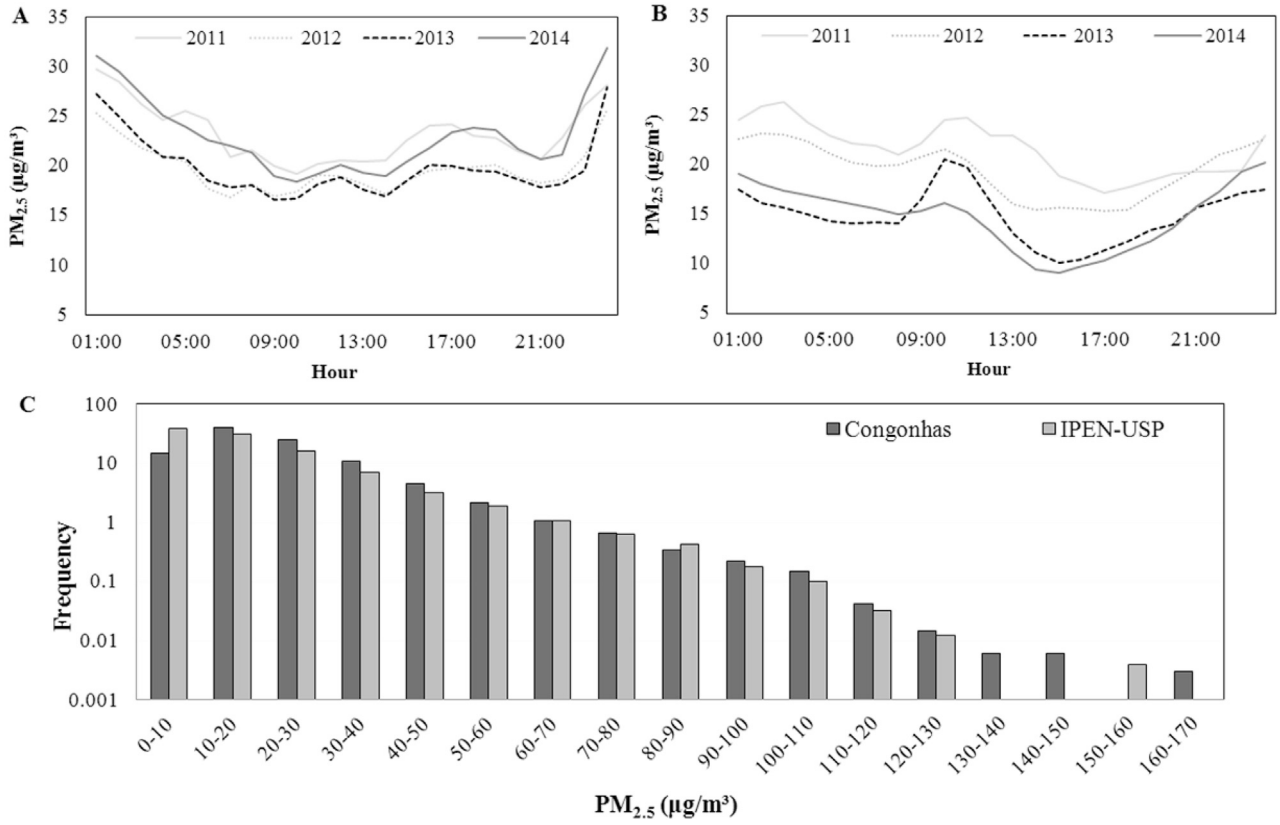

Fig. 7. Hourly $PM_{2.5}$ concentrations and their concentration-frequency distributions for 2011 to 2014 at (A) Congonhas and (B) IPEN-USP stations.

analyzed due to the availability and quality of dataset, the pollutant concentrations did not present a well-defined seasonal behavior, with O_3 presenting the highest return period for extreme concentrations among the analyzed pollutants. Comparing both megacities, MASP has higher concentrations for all pollutants analyzed, except for NO and PM_{10} during the summer. In addition, MASP shows higher probabilities for extreme events, when compared with MARJ, which means a shorter return period of high concentrations, being O_3 and $PM_{2.5}$ the ones of greatest concern.

The EVA approach can be used as a management tool, and the results obtained may be used to support management actions. Finally, it is also important to draw attention to the values recorded throughout the year in the regions, which are higher than those recommended by WHO, and therefore, can endanger the health of the population.

Acknowledgements

The authors would like to thank the National Council for Scientific and Technological Development (Conselho Nacional de Desenvolvimento Científico e Tecnológico - CNPq), processes 404104/2013-4 and 303491/2015-9, Araucaria Foundation (328/2014), FAPESP (NUANCE-SPS, project number 2008/58104-8), as well as the Coordination for the Improvement of Higher Education Personnel (Coordenação de Aperfeiçoamento de Pessoal de Nível Superior – CAPES). They would also like to thank the São Paulo Environmental Protection Agency (CETESB) and the State Environmental Institute (INEA) for providing the air quality dataset used in this paper.

Appendix A. Supplementary data

Supplementary data related to this article can be found at https://doi.org/10.1016/j.wace.2017.10.004.

References

Alvares, C.A., Stape, J.L., Sentelhas, P.C., Gonçalves, J.L.M., Sparovek, G., 2014. Koppen's climate classification map for Brazil. Meteorol. Z. 22 (6), 711–728.

Andrade, M.F., Miranda, R.M., Fornaro, A., Kerr, A., Oyama, B., Andre, P.A., Saldiva, P., 2012. Vehicle emissions and PM2.5 mass concentrations in six Brazilian cities. Air Qual. Atmos. Health 5, 79–88.

Andrade, M.F., Ynoue, R.Y., Freitas, E.D., Todesco, E., Vela, A.V., Ibarra, S., Martins, L.D., Martins, J.A., Carvalho, V.S.B., 2015. Air quality forecasting system for Southeastern Brazil. Front. Environ. Sci. 3 (9), 1–14.

Andrade, M.F., Kumar, P., Freitas, E.D., Ynoue, Y.R., Martins, J.A., Martins, L.D., Nogueira, T., Perez-Martinez, P., Miranda, R.M., Albuquerque, T., Gonçalves, F.L.T., Oyama, B., Zhang, Y., 2017. Air quality in the megacity of São Paulo: evolution over the last 30 years and future perspectives. Atmos. Environ. 159, 66–82.

Bautista, E.A.L.A., 2002. Distribuição Generalizada de Valores Extremos no Estudo da Velocidade Máxima do Vento em Piracicaba, SP. Universidade de São Paulo, Piracicaba.

Carvalho, V.S.B., Freitas, E.D., Martins, L.D., Martins, J.A., Mazzoli, C.R., Andrade, M.F., 2015. Air quality status and Trends over the metropolitan area of São Paulo, Brazil as a result of emission control policies. Environ. Sci. Policy 47, 68–79.

CETESB, 2017. Relatório de qualidade do ar no Estado de São Paulo 2016, São Paulo, p. 198. Air quality report for the São Paulo state, 2016 – São Paulo.

Comrie, A.C., Yarnal, B., 1992. Relationships between synoptic-scale atmospheric circulation and ozone concentrations in metropolitan pittsburgh, Pennsylvania. Atmos. Environ. Part B 26 (3), 301–312.

Cooper, O.R., Langford, A.O., Parrish, D., Farrey, D.W., 2015. Challenges of a lowered U.S. ozone standard. Science 348, 1096–1097.

Dominutti, P.A., Nogueira, T., Borbon, A., Andrade, M.F., Fornaro, A., 2016. One-year of NMHCs hourly observations in Sao Paulo megacity: meteorological and traffic emissions effects in a large ethanol burning context. Atmos. Environ. 142, 371–382.

Ercelebi, S.G., Toros, H., 2009. Extreme value analysis of istanbul air pollution data. Clean. – Soil Air Water 37 (2), 122–131.

Fisher, R.A., Tippett, L.H.C., 1928. Limiting forms of the frequency distribution of the largest or smallest member of a sample. Math. Proc. Camb. Philos. Soc. 24 (2), 180–190.

Freitas, E.D., Rozoff, C.M., Cotton, W.R., Silva Dias, P.P., 2007. Interactions of an urban heat island and sea breeze circulations during winter over the metropolitan area of Sao Paulo, Brazil. Boundary Layer Meteorol. 122 (1), 43–65. https://doi.org/10.1007/s10546-006-9091-3.

Georgopoulos, P.G., Seinfeld, J.H., 1982. Statistical distributions of air pollutant concentrations. Environ. Sci. Technol. 16 (7), 401A–416A.

Gioda, A., Ventura, L.M.B., Ramos, M.B., Silva, M.P.R., 2016. Half Century Monitoring Air Pollution in a Megacity: a Case Study of Rio de Janeiro. Water Air & Soil Pollut. 227, 86–102.
INEA, 2011. Relatório da qualidade do ar do Estado do Rio de Janeiro – ano base 2010 e 2011, p. 140, 2011. Rio de Janeiro.
IPCC, 2014. Climate change 2014: impacts, adaptation, and vulnerability. Part A: global and sectoral aspects. Contribution of working group II to the fifth assessment report of the intergovernmental panel on climate change. In: Field, C.B., Barros, V.R., Dokken, D.J., Mach, K.J., Mastrandrea, M.D., Bilir, T.E., Chatterjee, M., Ebi, K.L., Estrada, Y.O., Genova, R.C., Girma, B., Kissel, E.S., Levy, A.N., MacCracken, S., Mastrandrea, P.R., White, L.L. (Eds.). Cambridge University Press, Cambridge, United Kingdom and New York, NY, USA, p. 1132.
Jenkin, M.E., Davies, T.J., Stedman, J.R., 2002. The origin and day-of-week dependence of photochemical ozone episodes in the UK. Atmos. Environ. 36 (6), 999–1012.
Jenkinson, A.F., 1955. .The frequency distribution of the annual maximum (or minimum) values of meteorological elements. Q. J. R. Meteorol. Soc. 81 (348), 158–171.
Küchenhoff, H., Thamerus, M., 1996. Extreme value analysis of munich air pollution data. Ecol. Stat. 3 (2), 127–141.
Kumar, P., Andrade, M.F., Ynoue, R.Y., Fornaro, A., Freitas, E.D., Martins, J.A., Martins, L.D., Albuquerque, T., Zhang, Y., Morawska, L., 2016. New directions: from biofuels to wood stoves: the modern and ancient air quality challenges in the megacity of São Paulo. Atmos. Environ. 140, 364–369. https://doi.org/10.1016/j.atmosenv.2016.05.059.
Lima, K.C., Satyamurty, P., Fernández, J.P.R., 2010. Large-scale atmospheric conditions associated with heavy rainfall episodes in Southeast Brazil. Theor. Appl. Climatol. 101, 121–135.
Loomis, D., Grosse, Y., Lauby-Secretan, B., Ghissassi, F.E., Bouvard, V., Benbrahim-Tallaa, L., Guha, N., Baan, R., Mattock, H., Straif, K., 2013. On behalf of the international agency for research on cancer monograph working group IARC, lyon. France. Lancet Oncol. 14 (13), 1262–1263.
Lu, H.C., 2004. Estimating the emission source reduction of PM_{10} in central Taiwan. Chemosphere 54 (7), 805–814.
Magrin, G.O., Marengo, J.A., Boulanger, J.-P., Buckeridge, M.S., Castellanos, E., Poveda, G., Scarano, F.R., Vicuña, S., 2014. Central and South America. In: climate change 2014: impacts, adaptation, and vulnerability. Part B: regional aspects. Contribution of working group II to the fifth assessment report of the intergovernmental panel on climate change. In: Barros, V.R., Field, C.B., Dokken, D.J., Mastrandrea, M.D., Mach, K.J., Bilir, T.E., Chatterjee, M., Ebi, K.L., Estrada, Y.O., Genova, R.C., Girma, B., Kissel, E.S., Levy, A.N., MacCracken, S., Mastrandrea, P.R., White, L.L. (Eds.). Cambridge University Press, Cambridge, United Kingdom and New York, NY, USA, pp. 1499–1566.
Martins, L.D., Andrade, M.F., 2008. ozone formation potentials of volatile organic compounds and ozone sensitivity to their emission in the megacity of São Paulo, Brazil. Water Air & Soil Pollut. 195 (1), 201–213.
Martins, L.D., Martins, J.A., Freitas, E.D., Mazzoli, C.R., Gonçalves, F.L.T., Ynoue, R.Y., Hallak, R., Alburquerque, T.T.A., Andrade, M.F., 2009. Potential health impact of ultrafine particles under clean and polluted urban atmospheric conditions: a model-based study. Air Qual. Atmos. Health 29–39.
Martins, E.M., Nunes, A.C.L., Corrêa, S.M., 2015. Understanding ozone concentrations during weekdays and weekends in the urban area of the city of Rio de Janeiro. J. Braz. Chem. Soc. 26 (10), 1967–1975.
Mateus, V., Monteiro, I., Rocha, R., Saint'Pierre, T., Gioda, A., 2013. Study of the chemical composition of particulate matter from Rio de Janeiro metropolitan region, Brazil, by inductively coupled plasma-mass spectrometry and optical emission spectrometry. Spectrochim. Acta Part B 86, 131–136.
McNeil, A.J., Saladin, T., 1997. The Peaks over Thresholds Methods for Estimating High Quantiles of Loss Distributions. Accessed in 30 August 2017. http://citeseerx.ist.psu.edu/viewdoc/download?doi=10.1.1.71.8466&rep=rep1&type=pdf.
Panagoulia, D., Economou, P., Caroni, C., 2014. Stationary and nonstationary generalized extreme value modelling of extreme precipitation over a mountainous area under climate change. Environmetrics 25, 29–43.
Paulino, S.A., Quiterio, S.L., Escaleira, V., Arbilla, G., 2010. Evolution of particulate matter and associated metal levels in the urban area of Rio de Janeiro, Brazil. Bull. Environ. Contam. Toxicol. 84, 315–318.
Pereira, G.M., Alves, N.D.O., Caumo, S.E.S., Soares, S., Teinilä, K., Custódio, D., Hillamo, R., Alves, C., Vasconcellos, P.C., 2017. Chemical composition of aerosol in São Paulo, Brazil: influence of the transport of pollutants. Air Qual. Atmos. Health 10, 457–468.
Pickands, J., 1975. Statistical inference using extreme order statistics. Ann. Stat. 3 (1), 119–131.
Piegorsch, W.W., Smith, E.P., Edwards, D., Smith, R.L., 1998. Statistical advances in environmental science. Stat. Sci. 13 (2), 186–208.
Quintela-Del-Río, A., Francisco-Fernández, M., 2011. Nonparametric functional data estimation applied to ozone data: prediction and extreme value analysis. Chemosphere 82 (6), 800–808.
Ravishankara, A.R., 2005. Chemistry-climate coupling; the importance of chemistry in climate issues (Introductory Lecture). Faraday Discuss. Chem. Soc. 130, 9–25. https://doi.org/10.1039/b509603k.
Roberts, E.M., 1979. Review of statistics of extreme values with applications to air quality data. J. Air Pollut. Control Assoc. 29 (7), 733–740.
Sánchez-Ccoyllo, O.R., Ynoue, R.Y., Martins, L.D., Andrade, M.F., 2006. Impacts of ozone precursor limitation and meteorological variables on ozone concentration in São Paulo, Brazil. Atmopheric Environ. 40 (2), 552–562.
Sangisolo, C.A., 2008. Distribuições de Extremos de Precipitação Diária, Temperatura Máxima e Mínima e Velocidade do Vento em Piracicaba, SP (1917-2006). Rev. Bras. Meteorol. 23 (3), 341–346.
Sharma, P., Khare, M., Chakrabarti, S.P., 1999. Application of extreme value theory for predicting violations of air quality standards for an urban road intersection. Transp. Res. 4 (3), 201–216.
Silva Dias, M.A.F., Dias, J., Carvalho, L.M.V., Freitas, E.D., Silva Dias, P.L., 2013. Changes in extreme daily rainfall for São Paulo, Brazil. Clim. Change 116, 705–722.
Smith, R.L., 1989. Extreme value analysis of environmental time series: an application to trend detection in ground-level ozone. Stat. Sci. 4 (4), 367–377.
Su, F.C., Jia, C., Batterman, S., 2012. Extreme value analyses of VOC exposures and risks: a comparison of RIOPA and NHANES datasets,. Atmos. Environ. 62, 97–106.
United Nations, Department of Economic and Social Affairs, Population Division, 2014. World Urbanization Prospects: the 2014 Revision.
United Nations, Department of Economic and Social Affairs, Population Division, 2016. The World's Cities in 2016 – Data Booklet (ST/ESA/SER.A/392).
Xing, Y.-F., Xu, Y.-H., Shi, M.-H., Lian, Y.-X., 2016. The impact of $PM_{2.5}$ on the human respiratory system. J. Thorac. Discuss. 8, E69–E74.
Weibull, W., 1951. A statistical distribution function of wide applicability. J. Appl. Mech. 293–299.
World Health Organization, 2013. Review of Evidence on Health Aspects of Air Pollution – REVIHAAP Project. Technical Report, p. 309. Denmark, 2013.